

Supplementary Material

Projected drought risk in 1.5°C and 2°C warmer climates

Flavio Lehner¹, Sloan Coats², Thomas F. Stocker^{3,4}, Angeline G. Pendergrass², Benjamin M. Sanderson², Christoph C. Raible^{3,4}, Jason E. Smerdon⁵

¹Research Applications Laboratory, National Center for Atmospheric Research, Boulder, USA

²Climate and Global Dynamics Laboratory, National Center for Atmospheric Research, Boulder, USA

³Oeschger Centre for Climate Change Research, University of Bern, Bern, Switzerland

⁴Climate and Environmental Physics, University of Bern, Bern, Switzerland

⁵Lamont-Doherty Earth Observatory of Columbia University, Palisades, NY, USA

Corresponding author: Flavio Lehner (flehner@ucar.edu)

Content

- Comparison of Drought Atlas and preindustrial control simulation
- Figures S1-S11

Comparison of Drought Atlas and preindustrial control simulation

The CESM preindustrial control simulation generally shows good agreement with the Drought Atlases (Figure S4). Notable differences in specific PDSI bins occur in the Mediterranean, the Central Plains, and Southeast Asia, where the distribution of the Drought Atlases is slightly wider than in CESM. Thus, to the extent that CESM and reconstruction are comparable and to the extent that preindustrial model biases project onto future projections, the model might underestimate future drought risk in those particular regions. The missing variability in the model compared to the Drought Atlases could be a function of missing preindustrial forcings in CESM, such as volcanoes or solar irradiance variations, which are absent in the preindustrial control simulation.

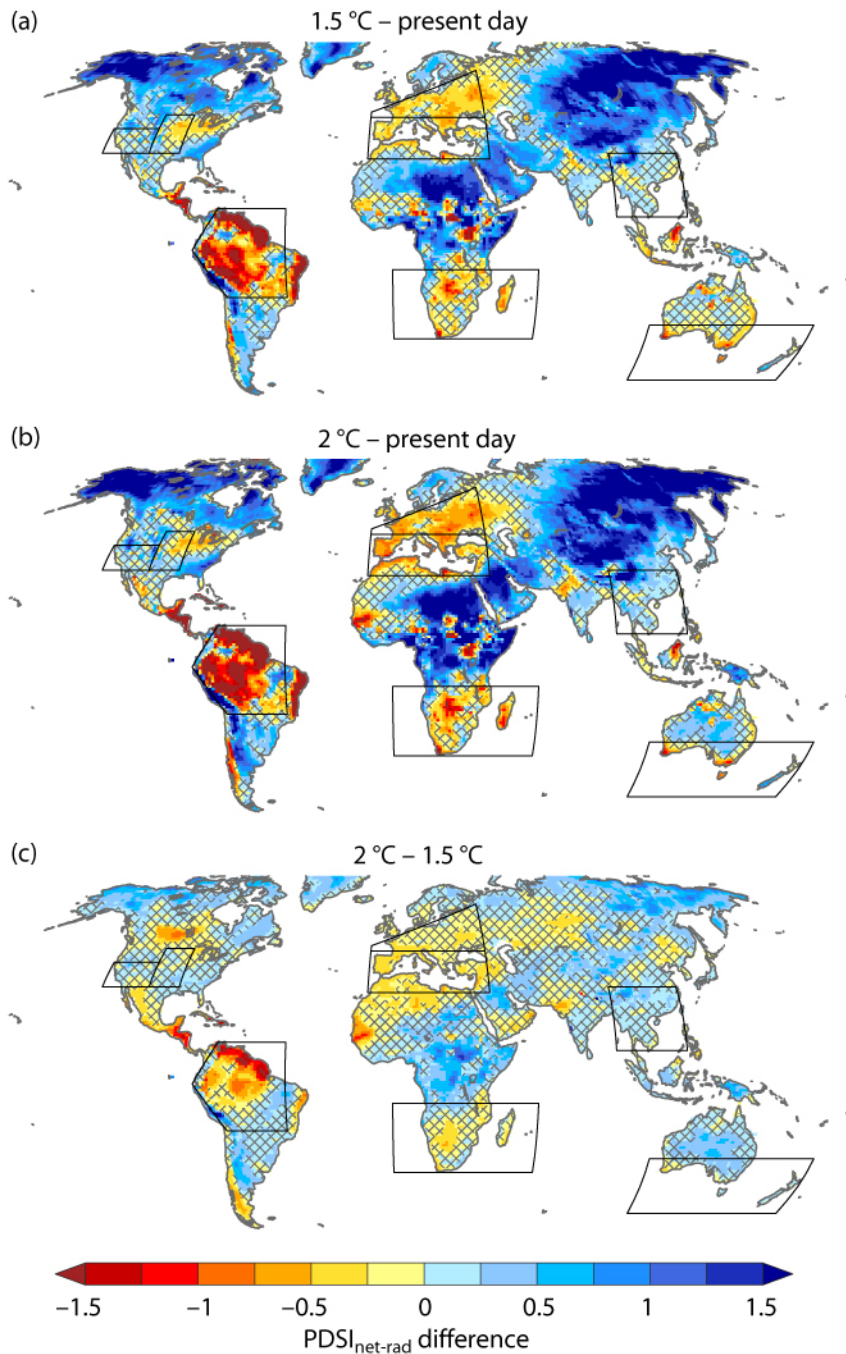


Figure S1. Change in mean PDSI_{net-rad} **(a)** from present day to 1.5°C, **(b)** from present day to 2°C, **(c)** from 1.5°C to 2°C, as simulated by CESM. Hatching indicates differences that are not significant according to a two-sided *t*-test with 95% confidence.

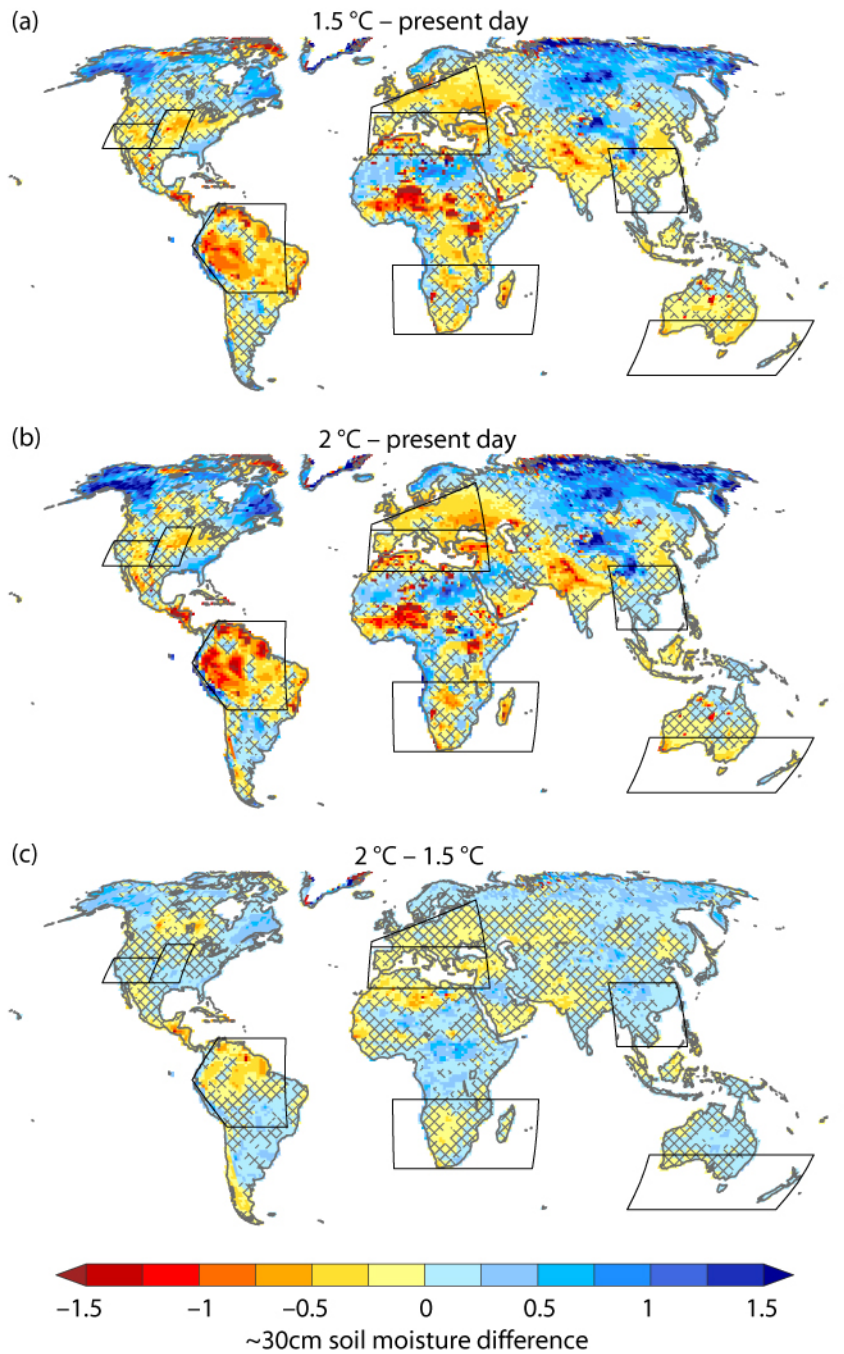


Figure S2. Change in normalized ~30cm integrated soil moisture **(a)** from present day to 1.5°C, **(b)** from present day to 2°C, **(c)** from 1.5°C to 2°C, as simulated by CESM. Hatching indicates differences that are not significant according to a two-sided *t*-test with 95% confidence.

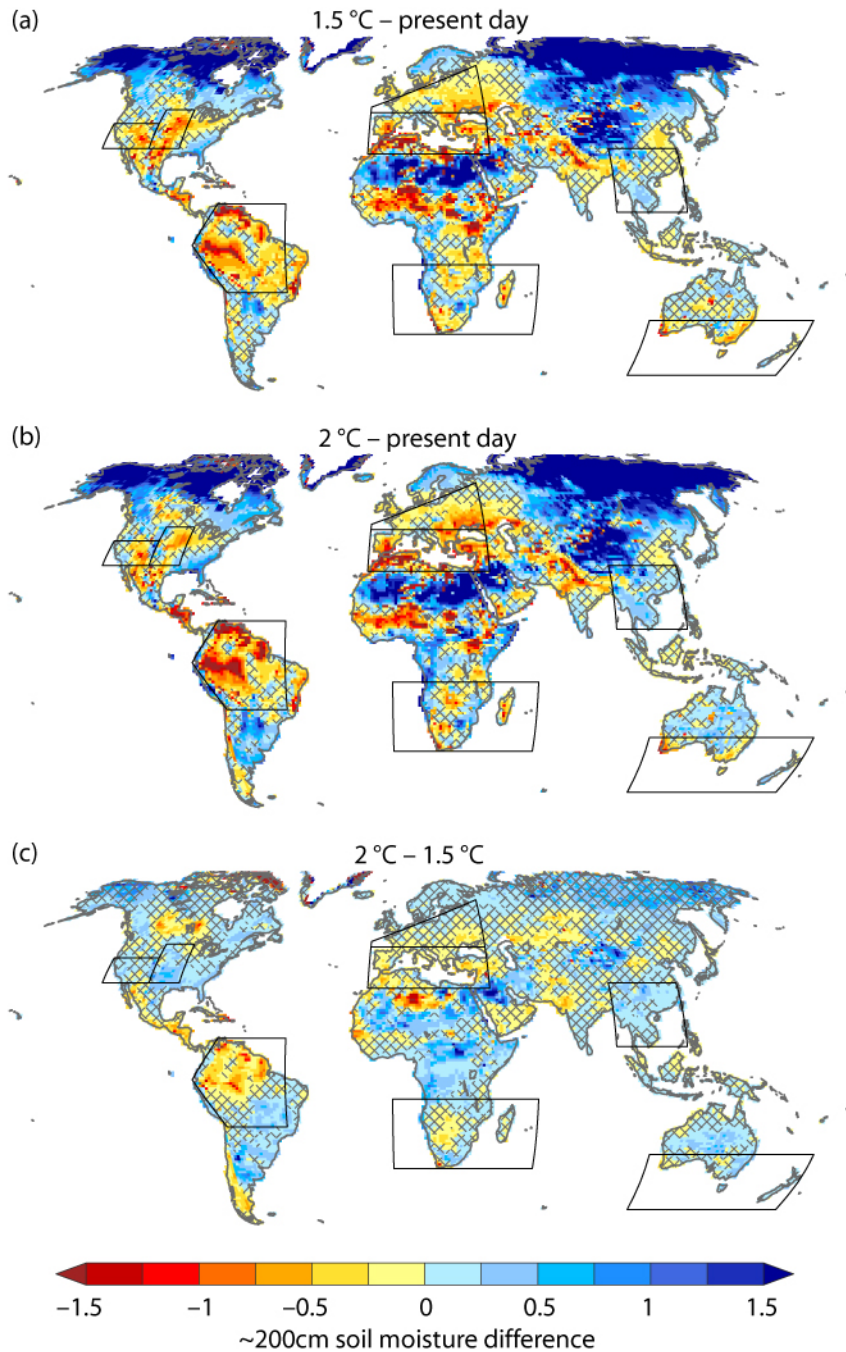


Figure S3. Change in normalized ~200 cm integrated soil moisture **(a)** from present day to 1.5°C, **(b)** from present day to 2°C, **(c)** from 1.5°C to 2°C, as simulated by CESM. Hatching indicates differences that are not significant according to a two-sided *t*-test with 95% confidence.

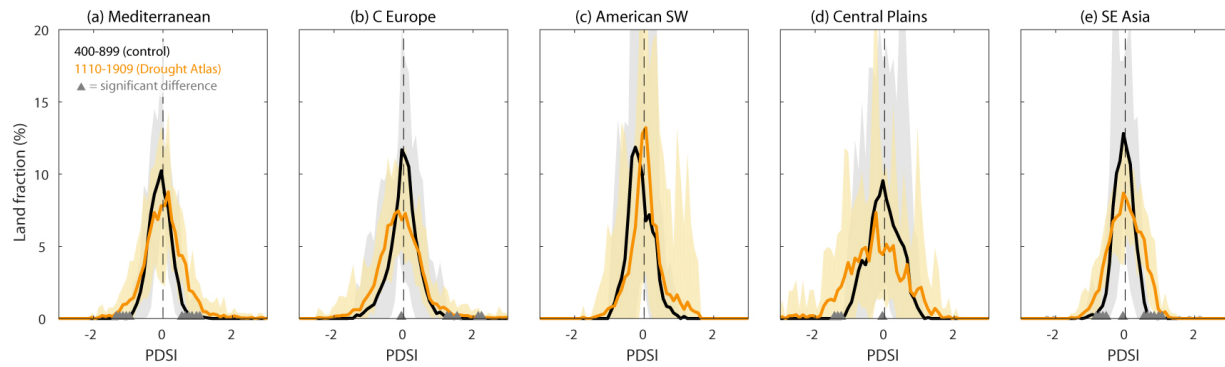


Figure S4. 50-year mean PDSI from the CESM preindustrial control simulation and the different Drought Atlases (where available) as a function of land fraction for (a) the Mediterranean, (b) Central Europe, (c) American Southwest, (d) US Central Plains, and (e) Southeast Asia. Drought Atlases: (a-b) Old World Drought Atlas (Cook et al. 2015), (c-d) North American Drought Atlas (Cook et al. 2004), and (e) Monsoon Asia Drought Atlas (Cook et al. 2010). Each thick solid line is the mean of the corresponding consecutive and non-overlapping 10 (control) or 16 (Drought Atlases) 50-year periods; the shading shows the full range across those values. Gray triangles indicate significant difference at 95% confidence. PDSI from the preindustrial control simulation is standardized against its full length, while the Drought Atlases are standardized against 1931-1990; in practice, both are essentially centered on zero, indicating the robustness of PDSI between the model and reconstructions.

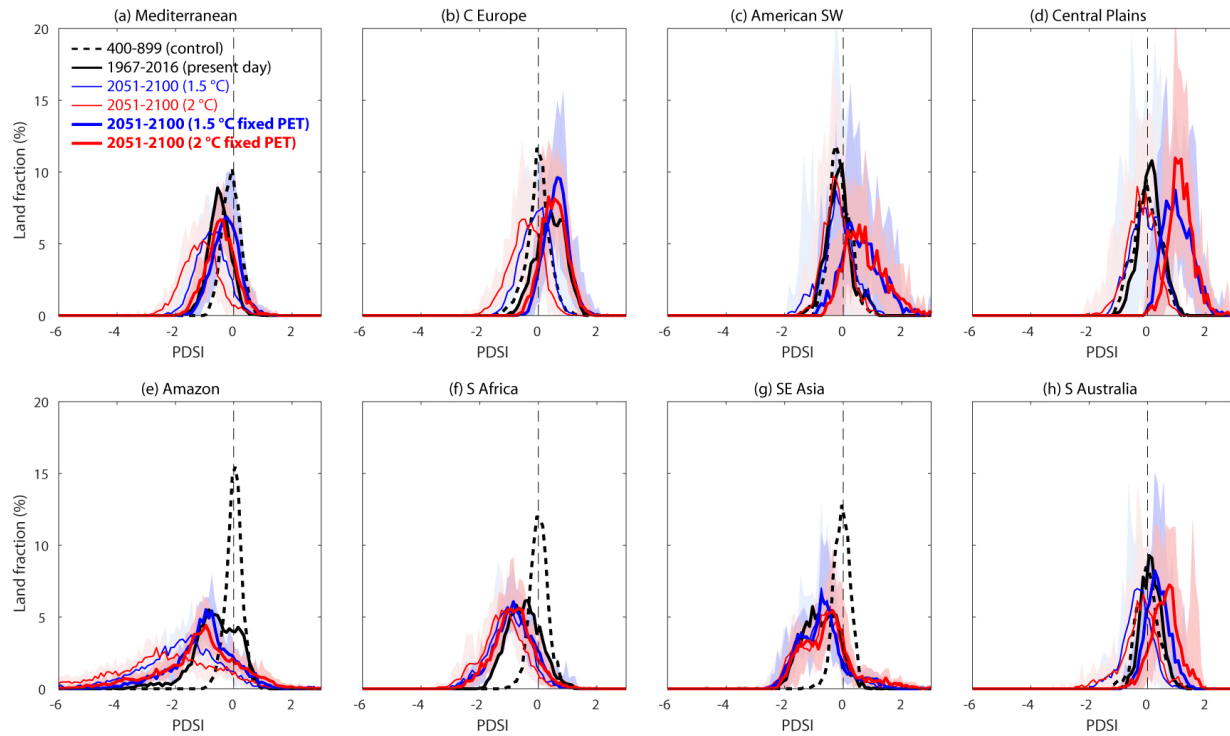


Figure S5. Following Figure 2, comparison of PDSI at 1.5°C and 2°C warming calculated with potential evapotranspiration (PET) detrended quadratically (thick colored lines) and without detrending (thin colored lines; see text for details). Also shown are the ensemble mean of the preindustrial control (black dashed) and historical (black solid) simulations. Shading indicates the full range across ensemble members; omitted from the control and present day for clarity.

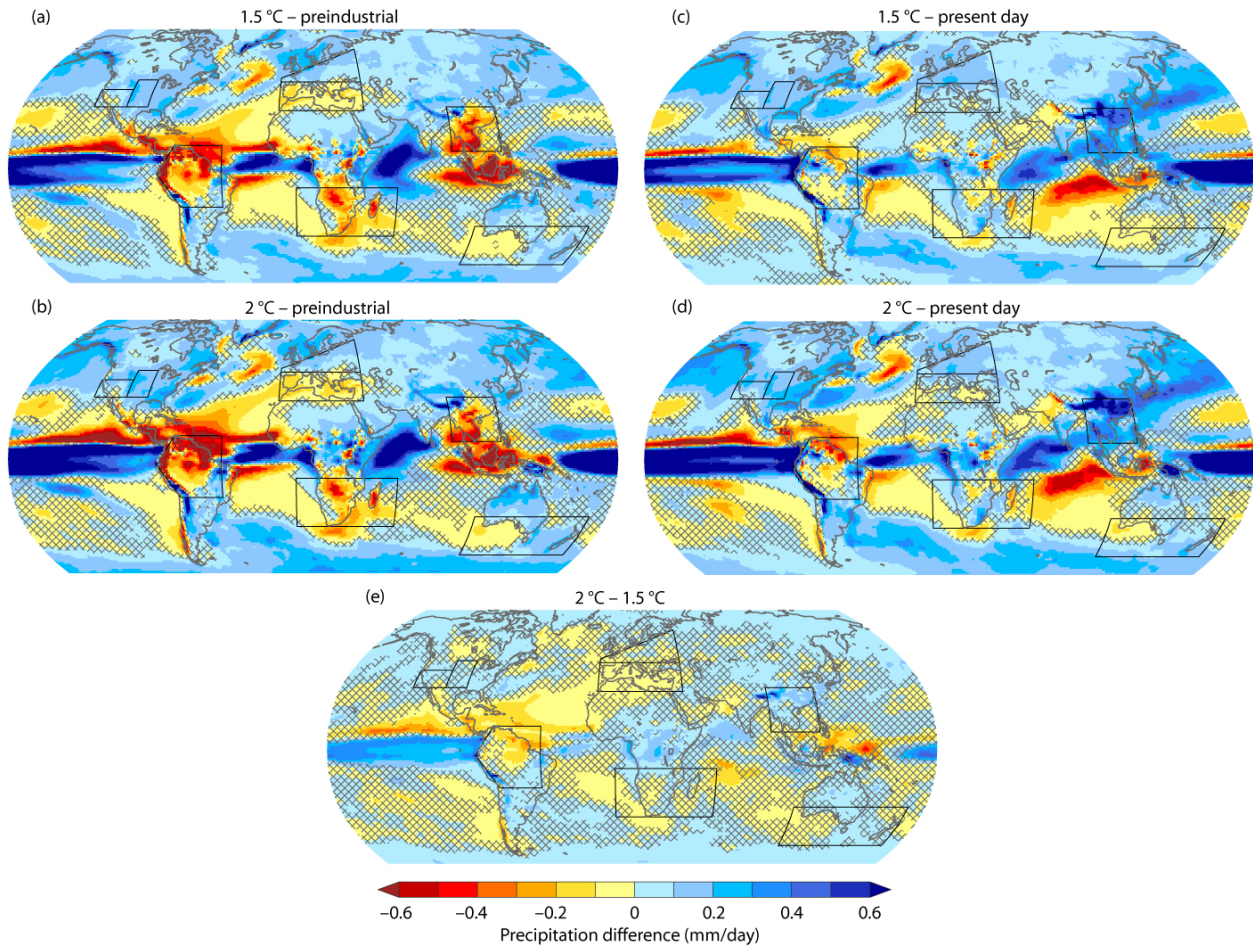


Figure S6. Change in precipitation (a) from preindustrial to 1.5°C, (b) from preindustrial to 2°C, (c) from present day to 1.5°C, (d) from present day to 2°C, and (e) from 1.5°C to 2°C, as simulated by CESM. Hatching indicates differences that are not significant according to a two-sided *t*-test with 95% confidence.

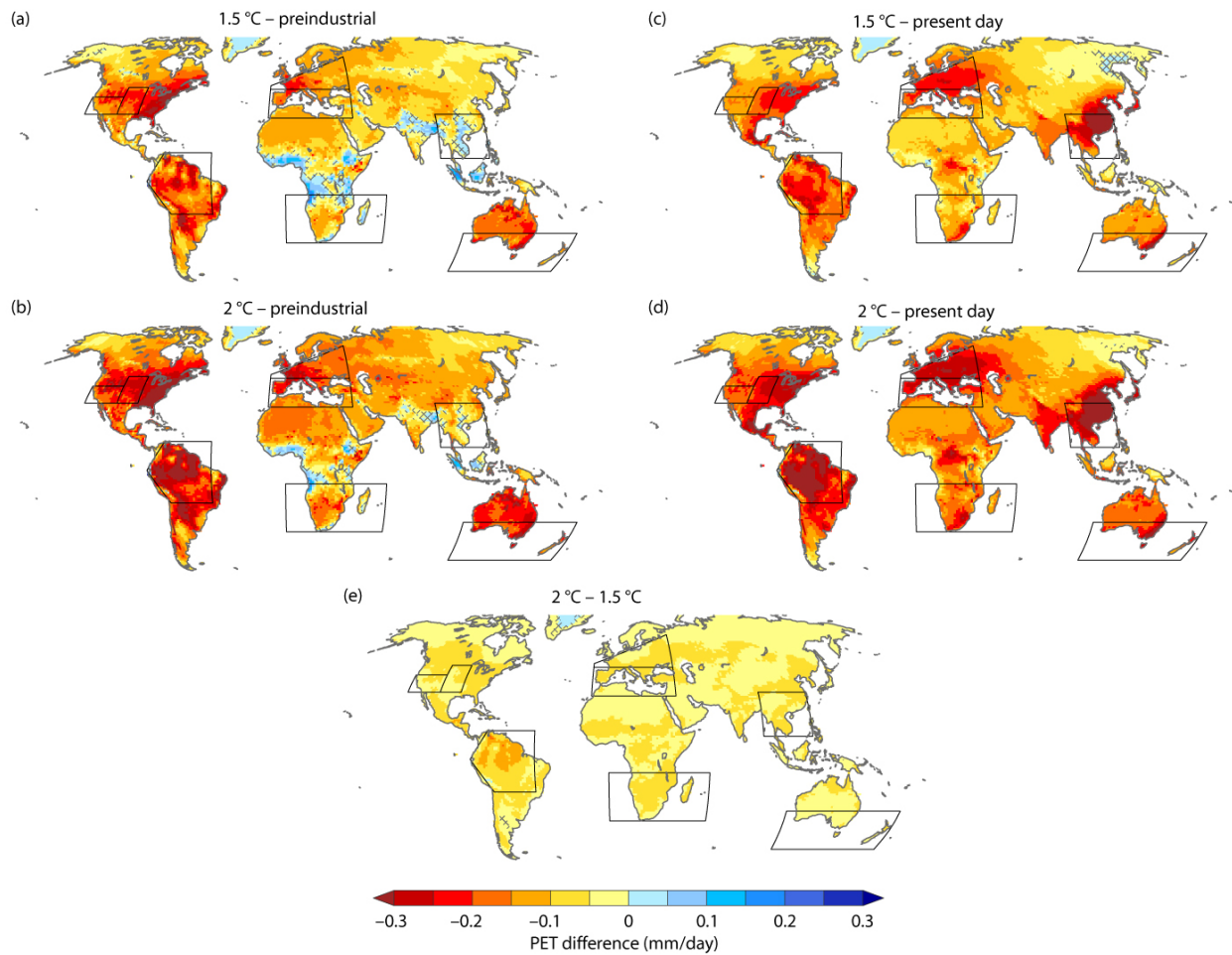


Figure S7. Change in potential evapotranspiration (PET) (a) from preindustrial to 1.5°C, (b) from preindustrial to 2°C, (c) from present day to 1.5°C, (d) from present day to 2°C, and (e) from 1.5°C to 2°C, as simulated by CESM. Hatching indicates differences that are not significant according to a two-sided *t*-test with 95% confidence.

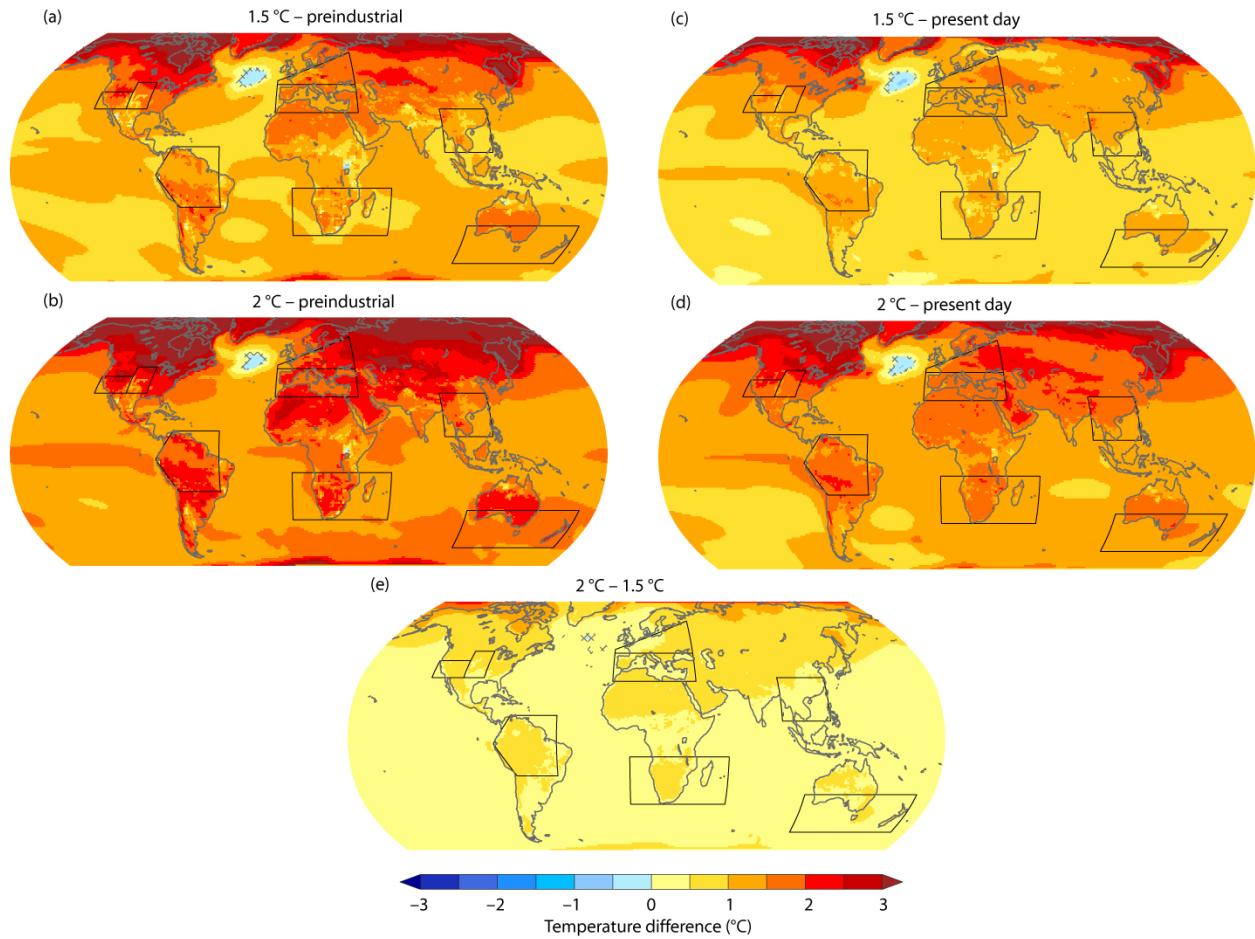


Figure S8. Change in surface air temperature (a) from preindustrial to 1.5°C, (b) from preindustrial to 2°C, (c) from present day to 1.5°C, (d) from present day to 2°C, and (e) from 1.5°C to 2°C, as simulated by CESM. Hatching indicates differences that are not significant according to a two-sided *t*-test with 95% confidence.

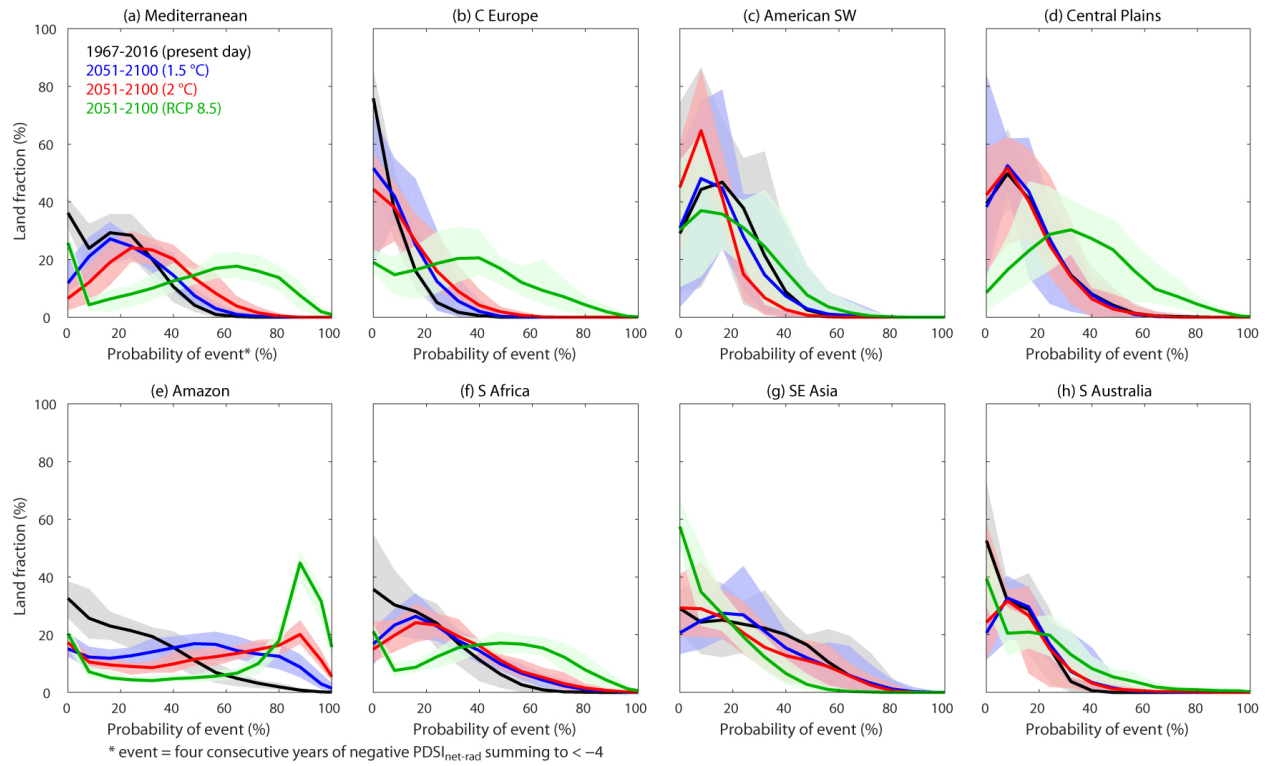


Figure S9. Risk (probability of occurrence) of four consecutive years with negative $PDSI_{net-rad}$ summing to less than -4 as a function of land fraction for the same regions as in Figs. 2-3. Probability of occurrence is calculated as the number of events divided by the maximum number of possible non-overlapping events in a 50-year period. Shading indicates the full range across ensemble members.

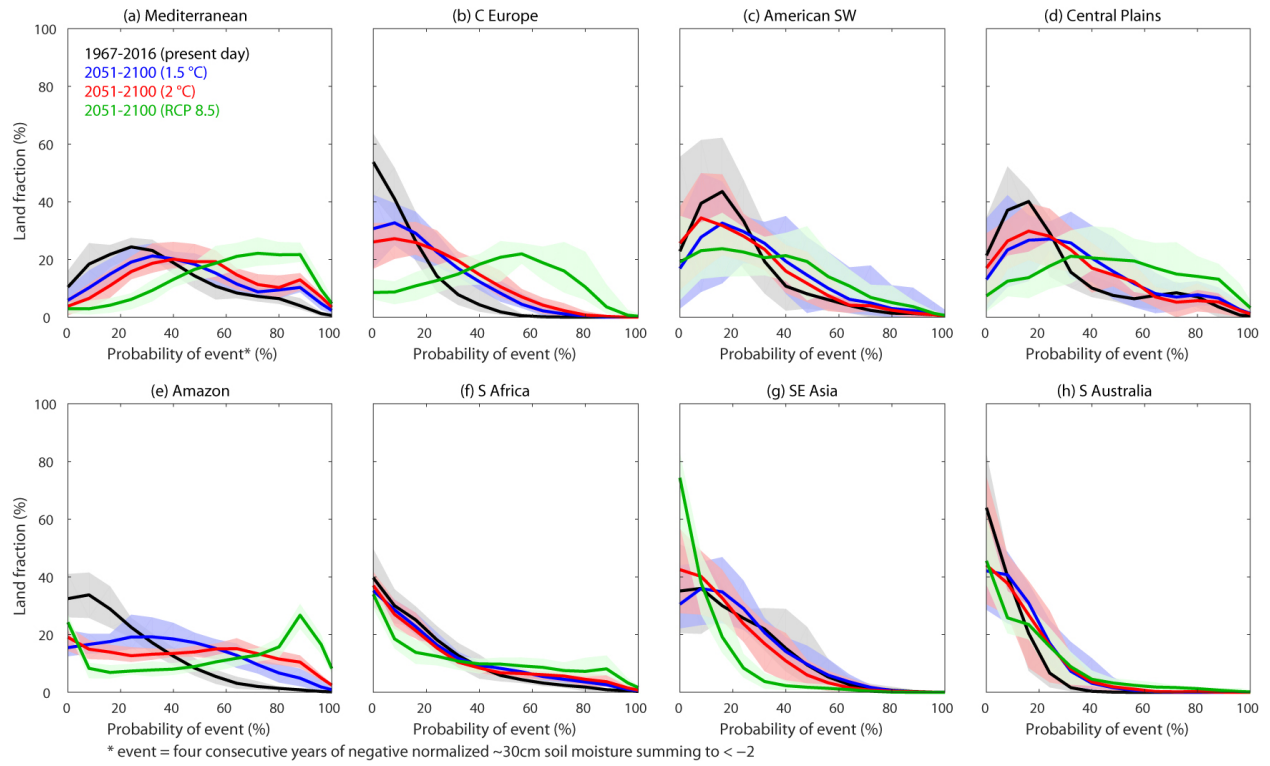


Figure S10. Risk of four consecutive years with normalized ~30cm soil moisture summing to < -2 as a function of land fraction for the same regions as in Figs. 2-3, following Fig. S9. The threshold of -2 for a four-year sum corresponds roughly to PDSI of -4 .

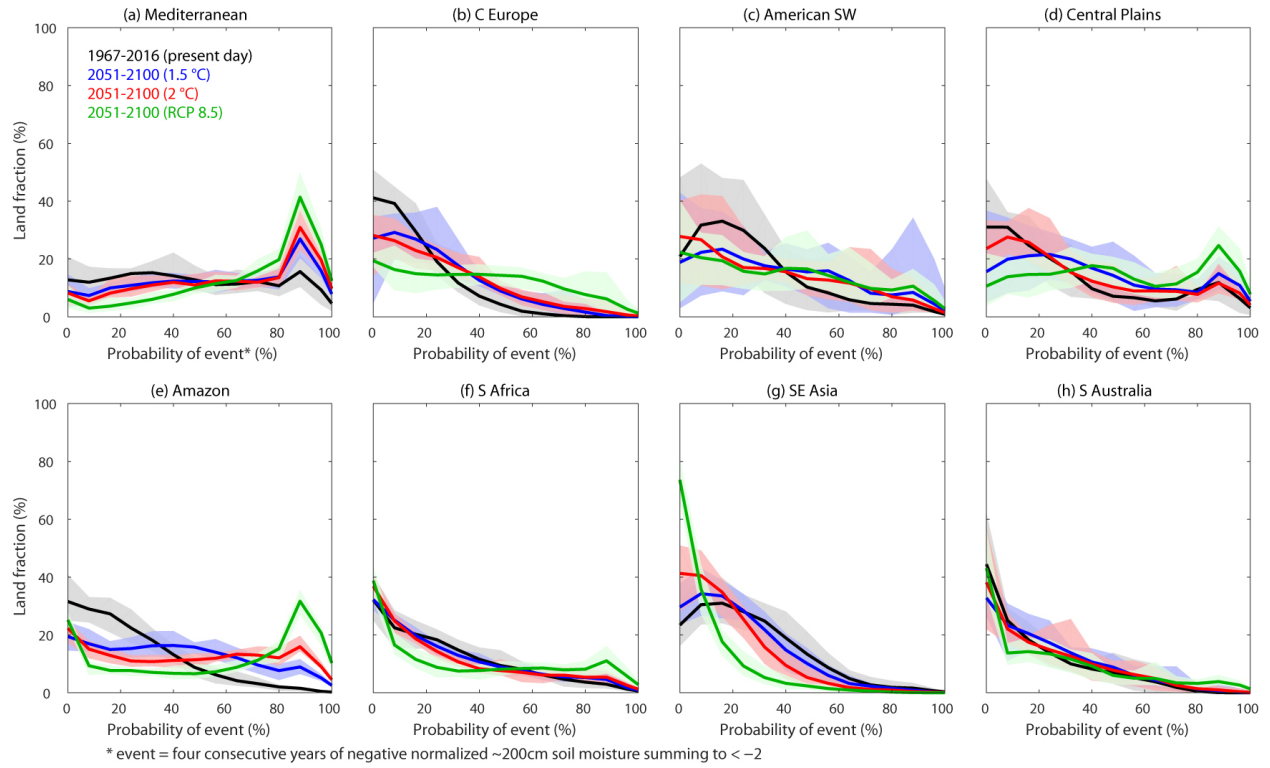


Figure S11. Risk of four consecutive years with normalized ~200cm soil moisture summing to < -2 as a function of land fraction for the same regions as in Figs. 2-3, following Fig. S10.